CrossMark

ORIGINAL PAPER

Using FEM simulation to predict structural performances of a sailing dinghy

A. Mancuso[1] · G. Pitarresi[1] · D. Tumino[2]

Abstract The use of finite element method (FEM) tools is proposed to investigate the structural response of an eco-sustainable sailing yacht to different loading conditions, typical of those acting during regattas. The boat is, in particular, a 4.60 m dinghy with the hull and the deck made of an hybrid flax–cork sandwich and internal reinforcements made of marine plywood. A preliminary activity has consisted in the refitting of an existing model in order to reduce the hull weight and to improve performances during manoeuvrings. These tasks have been interactively simulated in the virtual environment of the boat CAD model, where longitudinal and transversal reinforcements were enlightened and the maximum beam reduced. At the same time, results of FEM simulations on the modified model were analysed in order to verify the structural integrity. Shape modifications have been applied to the real model in laboratory and the resulting hull has been instrumented with strain gauges and tested under rigging conditions to validate the numerical procedure. Finally, the FEM model was used to predict the response of the boat to loading systems typical of sailing conditions.

Keywords Refitting · Sailing yacht · FEM

✉ D. Tumino
davide.tumino@unikore.it

1 Dipartimento dell'Innovazione Industriale e Digitale, DIID, Università degli Studi di Palermo, Viale delle Scienze, 90128 Palermo, Italy

2 Università degli Studi di Enna Kore, Facoltà di Ingegneria e Architettura, Cittadella Universitaria, 94100 Enna, Italy

1 Introduction

Nowadays, yacht design methodologies make use of virtual tools able to predict most of the yacht performances from several standpoints. A CAD model, for instance, can be transformed to FEM or CFD models and virtually analysed to evaluate structural and fluid dynamic performances. Then, the analysis of the obtained numerical results can give useful hints about changes to be applied to the CAD model, in terms of shape, topology or other design parameters. If a structured design approach is followed [1,2], these modifications become easily applicable until satisfactory results are achieved. Of course, the accurate estimation of rigging loads (internal) and aero/hydro loads (external) becomes a necessary condition for reasonable results. The internal load system depends on rigging specifications (e.g. with or without spreaders, fractional) and can be found by solving the related force equilibrium equations. An accurate prediction of the external load system is instead much more complex, usually requiring days for running a single CFD simulation [3]. As a matter of course, this methodology is applied in the competition field (e.g. America's Cup, Volvo Ocean race, Vendeè Globe), while, as a general rule, the design processes of series products make use of International Standards (ISO, RINA, etc.) in place of more time (and cost) consuming numerical simulations.

Several works have been found concerning the design of mid-large racing yachts. For instance in [4] the problem of the load growth (external load system) due to slamming effect on a large Open 60' is experimentally approached on field and in laboratory; while in [5] a numerical procedure is prosed to sketch the topology of a large oceanic yacht subjected to rigging loads only. A Stochastic Finite Element Analysis is proposed in [6] always for a large oceanic yacht focusing on the estimation and influence of uncertainties associated

to some variables (fibre orientation, mechanical properties, etc.) which can cause deviation from the estimated response. In [7] particular attention has been paid on the determination of the longitudinal strength of a large sloop sailing yacht subjected to hogging and sagging conditions, comparing a simplified analytical method with FEM results. Finally, the scantling process of rigging and mast is examined in [8] for a 45' sailing yacht by means of FEM tools and dimensioning rules, while in [9] a similar topic is approached for a 40' racing yacht using an Analytical Hierarchy Process (AHP) and comparing results with FEM. In all these papers, it is demonstrated that, for large dimension yachts, FEM tools can be considered a useful and affordable support during the design process also with the aim to overcome conservative criteria usually given by naval standards and rules. In some cases, also experimental validation via fiber-optic sensors has been attempted like in [10] where the integrity of a IACC yacht is monitored.

When dealing with small boats such as dinghies, as in the present paper, much less information is available in literature. Most authors have spent much effort to predict performances of sailing dinghies via Velocity Prediction Programs (VPP). In [11], a sail depowering coefficient is one of the parameters added to standard VPPs in order to predict the speed of a dinghy. In [12] the effect of heel and trim angles has been systematically examined with CFD simulations and with experiments in towing tank to obtain a database to be implemented in a VPP model. An advanced VPP model is presented in [13] where the VPP model developed by the authors and applied to a Moth also considers the foil deflection and the crew position. These parameters are experimentally measured respectively with Digital Image Correlation techniques and with digital optical techniques of shape recognition. To the authors knowledge, the use of numerical FEM simulations to determine the strain state in the hull panels and in the reinforcements of a sailing dinghy has not been proposed yet.

In this work, the re-engineering of a 15' SKIFF sailing yacht is performed. SKIFF stands for Sail Keep It Flat and Fast. Such a kind of yacht exhibits the best performances when running flat on the sea (without heel) and trimmed lightly backward depending on wind intensity. A CAE (Computer Aided Engineering) methodology has been applied based on the complete integration between numerical estimation and experimental results. The CAD model of the original yacht has been rebuilt in CREO Parametric for both an interactive parameter management and an easy integration with the FEM modeller ANSYS Workbench. The numerical model represents the hull (made with an environmentally friendly composite sandwich made with a Flax Reinforced Epoxy skin laminate and a natural cork core), the deck and internal frames (both made with marine plywood). A system of simplified loads based on rigging forces has been
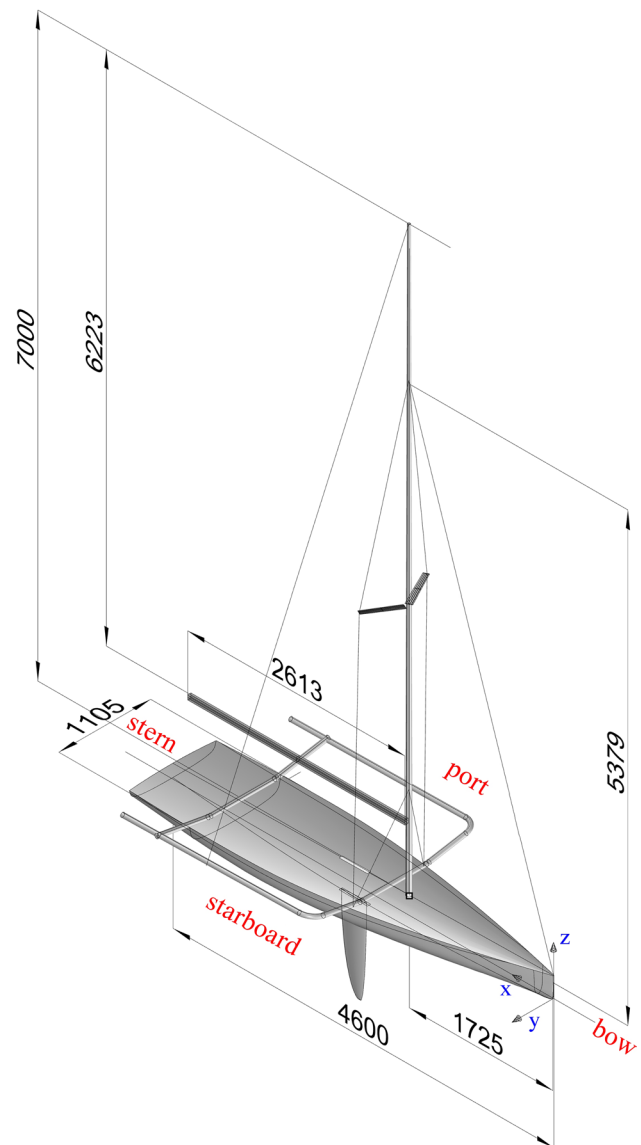

Fig. 1 Isometric view of LED with main dimensions

numerically studied and compared with results experimentally obtained by means of ER (Electrical Resistance) strain gauges installed in different locations of the hull and frame structure. LED, acronym of Linen Epoxy Dinghy, is the name of the boat analysed in this study and its virtual model is shown in Fig. 1.

2 Refitting

2.1 Virtual and physical refitting

The original CAD model of LED was built in the NURBS based software Rhinoceros. To enhance an interactive approach to the model during the re-shaping phase, the original CAD has been completely rebuilt in CREO Parametric
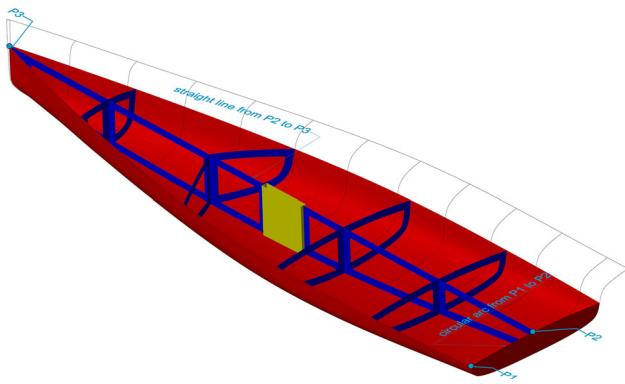
Fig. 2 Shaded view of the refitted version of LED compared with the original wireframe version

environment. This new generation of parametric solid modeller, widely used in several industrial engineering branches [14,15], gives the opportunity to virtually reproduce the technological procedures associated to the redesign of the model. In particular, Fig. 2 shows, with a solid black line, the original sections of the hull while the blue surfaces represent the final solution of the refitted hull and the internal frame. In order to speed up the manufacturing process, a developable surface has been chosen for the deck (hidden in Fig. 2). In fact, by sweeping the circular arc defined at stern by points P1 and P2 along the straight line defined by point P2 and P3, a developable surface is obtained. This geometry allows two different procedures to manufacture the deck: a composite sandwich structure can be obtained by lamination on an open mould and then joined to the hull but also a marine plywood cover can be easily cut along the toerail of the hull and then attached to it. One can note that the vertical positions of P2 and P3 on the longitudinal plane of symmetry define the freeboards at stern and bow, while the relative vertical distance between P1 and P2 defines the deck curvature in the transversal direction of the boat. According to crew feedback, the refitted boat has been modelled (and manufactured) with an opposite curvature of the deck with respect to the original one (convex surface instead of a concave one). Finally, the frame size (in terms of section height) provides a reference for the amount of material to be removed from the original sections and keel line. All these considerations have been transformed in mathematical constraints and parameters inside CREO for an easy regeneration of the model. The goal of the refitting phase was to reduce the weight of the dry boat and to improve its manoeuvrability by cutting and removing parts of the internal frame and hull. In particular, the reduction of the maximum beam leads to a reduction of the transverse moment of inertia and, as a consequence, to an improvement in performances during regattas.

Starting from the initial shape shown in Fig. 3 on the left, the final shape, obtained after an accurate FEM investigation (details are given in Sect. 3), is shown in Fig. 3 on the right.

In the original version of the boat, all transversal and longitudinal reinforcements were solid panels made of a 8 mm thick marine plywood, then these panels were drilled and cut in order to leave only 50 mm wide strips along the joints with the hull (see Fig. 3 left and right as comparison). The final weight of the refitted boat, measured in dry, off-water, conditions and with no armed rig, was 71 kg, i.e. 19% lighter than the original structure (weighing 88 kg).

2.2 Strain monitoring system

In order to validate the predictions of the numerical model with independent experimental measurements, some locations were selected as sites for bonding Electrical Resistance (ER) Strain Gages. Such locations were picked, after analyzing the FEM strain distribution, and are shown in Fig. 4. In particular, four points were chosen upon the hull sandwich (on the in-board side), and four other points on the wooden frame. The complex and a-priori unknown strain distribution on the hull points suggests the use of three-grid rosettes, in order to obtain principal strain components and principal strain directions relative to the outer lamina of the sandwich. Rectangular rosettes HBM RY81-6/350 were selected for the purpose. Regarding the points on the wood structure, these were monitored by single grid ER gages HBM LY11-6/350. In order to easily refer each measured result with the location where this is taken, an acronym nomenclature is propose, composed by three letters. In particular each measure is named XYZ, where: X is replaced by S for single grid ERs, or R for rosettes; Y is replaced by either K,W,B,S according if the ER is bonded on the Keel frame or Web frame, or the rosette is located on the Bow side or on the Stern side with respect to the mast; Z is replaced by S if the ER/rosette is on the Starboard side, or P if the ER/rosette is on the Port side. With this convention in place, four measures come for the stern side, i.e.: SKS, SWS, RBS, RSS, and four from the port side: SKP, SWP, RBP, RSP, with the two groups locations being symmetrically mirrored around the central beam keel. It must be mentioned that, when referring to the rosette measures, the above labels have the meaning of principal higher strain component, obtained by combining the three grids measures.

A four wires connection has been prepared for each ER installation. Due to the particular aggressive environment where the ER are located, they have been with a polyurethane paint HBM type PU120 and a silicone sealing layer HBM type SG250. One rosette and one single grid ER were also prepared for use as dummy gauges for temperature compensation on equivalent pieces of sandwich and plywood. The orientation for the rosettes was chosen such to try to obtain the same mutual alignment between the outer lamina fibres direction and the three grids. In doing so, it is though difficult

Fig. 3 View of LED without the deck: before refitting (*left*), after refitting (*right*)
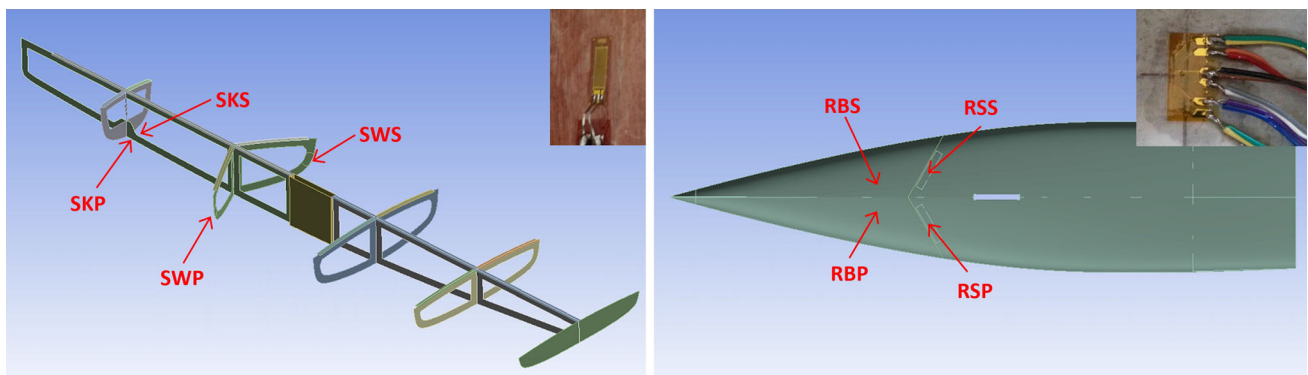

Fig. 4 Locations of strain gauges: single grids on reinforcements (*left*) and rosettes on the hull panels (*right*)

to avoid or carefully control misalignment errors. These are though not a concern in the calculation of principal strains from the three-grids measurements, as this is unaffected by the actual fibres alignment [16,17]. In light of this, the strain value chosen for comparison between the rosettes and the numerical prediction (reported in Sect. 3.4) is the maximum principal strain.

In order to simultaneously measure all signal from the four rosettes (equivalent to 12 grids) and the four ER grids, a HBM MGC PLUS data logger was used allowing for multi-channel acquisitions. Each grid was connected to a dedicated single channel, and each channel used a four wires quarter bridge connection scheme, allowing to compensate the effects of temperature on the wires resistance, and the drops of potential along the line. The dummy gauges were monitored through dedicated channels, in order to check for the presence of drifts due to temperature variations during the sampling. At this regard, it is reported that no significant temperature drift was detected by both the dummy and the active gauges, monitored in lab conditions for 20 minutes before applying the rigging load, with all signals oscillating within $\pm 1\,\mu\text{m/m}$.

3 Numerical simulations

A preliminary step consisted in the preparation of the complete CAD model of the boat in CREO Parametric (from PTC). All modifications to the original shape of LED have been virtually simulated in order to verify the feasibility of each procedure. Simulations have been performed in ANSYS r.15. Different modules of the package have been adopted, in particular: external aerodynamic forces have been calculated in FLUENT via CFD analysis to verify those carried out by analytical equations, ANSYS APDL has been used to resolve the forces and moments equilibrium of the boat, the orthotropic behaviour of the sandwich material [18,19] is modelled in the ACP PrePost and, finally, the structural response of the boat has been calculated in WORKBENCH via FEM analysis.

3.1 Estimation of loads

First aspect of this study is to determine the load system acting on the boat. In order to simplify the FEM model, the rig is not modelled but it is replaced by the load system that

Table 1 Loads [N] on rig

Configuration	Mast	Upwind shroud	Downwind shroud	Forestay
Rigging 1 (without deck)	−3000	1323	1323	387
Rigging 2 (with deck)	−3630	1600	1600	469
Navigation	−1991	−809	32	1235

the rig applies to the deck in correspondence of the point of junction of shrouds and mast with the deck. The rig is subjected to two different load systems: the first one is an internal self-equilibrated system and is obtained during compression preload (rigging) on the mast, as a consequence of this compression on the mast, shrouds and forestay are loaded under traction; the second load system is external to the boat and is represented by the hydro-aerodynamic forces and the weight of the crew members. The preload on the rig is applied before the boat is placed in the water and should not be modified during navigation. External loads are consequence of the aerodynamic loads and of the crew members location on the deck and change continuously during navigation.

After preload, the mast is subject to a pure compressive load, while shrouds and forestay to pure tension loads. Preload on mast, shrouds and forestay can be calculated by solving the equilibrium equations in a Cartesian reference system; this is a self-balanced system of forces necessary to compensate the load variations on the rig during navigation. Two values of preload on the mast have been applied, and the resulting rigging loads are then calculated and reported in Table 1. The sign of values reported in Table 1 refers to the prevalent action of the load: negative is for loads pushing the deck downward and positive for loads pulling the deck upward. The smaller preload (Rigging 1) is applied on the boat when the deck was not yet joined to the hull. The higher preload (Rigging 2) was applied when the boat was completed with the connection of the deck. The rigging forces are readily applied in the Workbench model at the connection points between the rig and the deck.

As stated above, the second load system takes into account the aerodynamic forces on sails, the hydrodynamic forces on hull and appendages and the crew weight [20].

In Fig. 5, the external forces acting in planes yz and xz are represented. Red arrows are the components of the resultant of the aerodynamic forces applied at the Center of Efforts (CE) of sails, green arrows are the components of the resultant of the hydrodynamic forces applied at the Center of Lateral Resistance (CLR) of the hull, the blue arrow is the resultant of the crew weight applied on trapeze. For the equilibrium around the y axis, moments have been calculated with respect to the center of buoyancy, see Fig. 5 left. Contributions of resistance forces on the bare hull and on the centreboard are neglected because of the small distance between the resultant

forces and the centre of buoyancy and because of the small values of these forces under the assumptions of low navigation speed. For the equilibrium around the x axis, moments have been calculated with respect to the centre of pressure on the centreboard, see Fig. 5 right.

The equilibrium of moments can be easily written as:

$$P \cdot b_{Px} = W_x \cdot b_{Wx,z} \qquad (1)$$
$$P \cdot b_{Py} = W_y \cdot b_{Wy,z} \qquad (2)$$

The crew weight is estimated as $P = 1500\,\text{N}$, while distances b_{Px} and b_{Py} can be determined from the geometry of the boat when the crew is on trapeze. An approximated value of $b_{Wy,z}$ (or similarly $b_{Wx,z}$) derives from the determination of the centroid of the jib and the main sail, see [20] for details. In particular, it has been found that the CE is about 3 m above the level of the deck. By solving Eqs. (1) and (2) the components of the aerodynamic force W have been found as $W_x = 230\,\text{N}$ and $W_y = 960\,\text{N}$.

Once the aerodynamic force on the rig is determined, it must be transferred on the deck. To do this, in the present paper, a simplified model of the rig has been modelled in the Mechanical APDL module of ANSYS by means of beam and link finite elements. Reactions on the junction points between the rig and the deck when the external load are applied are then numerically calculated and summarised in the third row of Table 1. This load system is the one coming from navigation conditions and can be added to the internal load system of rigging.

It is assumed that the boat runs flat during navigation. Pitch and heel are assumed to be zero in all simulations. The total weight of the boat (considering appendages and the rig) is 900 N and is applied as a volume distributed load. This weight, added to the crew weight, equals the displacement of the hull, $\nabla = 2400\,\text{N}$. In simulations presented in Sect. 4, the boat is supposed to be supported by an hydrostatic pressure distribution on the hull. It is assumed that this pressure distribution is not modified during navigation, although, in real conditions, also hydrodynamic effects should be taken into account. Nevertheless, this assumption is reasonable because of the low speed considered in the simulations (see Sect. 3.2 as comparison), conditions where dynamic pressure does not play a relevant role. Only when a pre-planning condition is simulated, the hydrostatic pressure distribution is deleted and the boat is assumed as supported at bow and stern on two wave peaks.

The last force to be considered on the boat is the one resulting from the hydrodynamic actions on the centerboard. Numerical techniques as inertia relief [21] are available in literature to evaluate this force; in this paper it has been calculated as reaction, applied on the trunk of the centerboard, able to equilibrate the above mentioned external loads and keeping the boat with a flat trim on the sea.

Fig. 5 Equilibrium of moments around y (*left*) and around x (*right*)
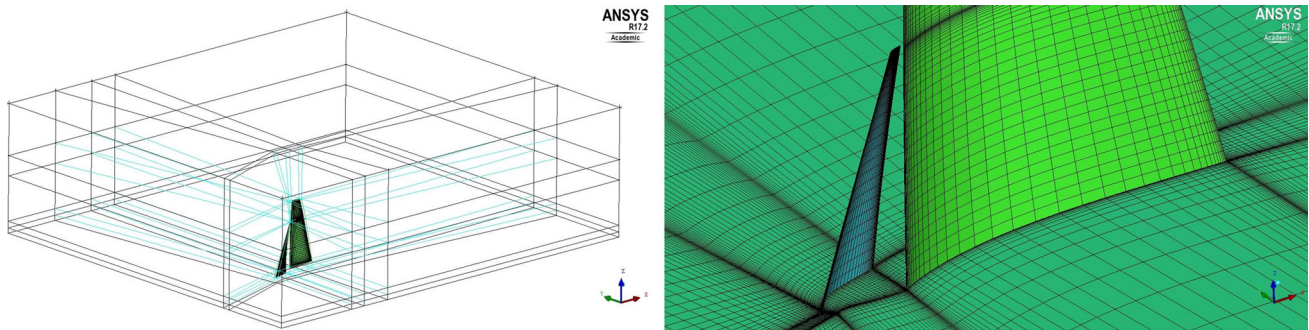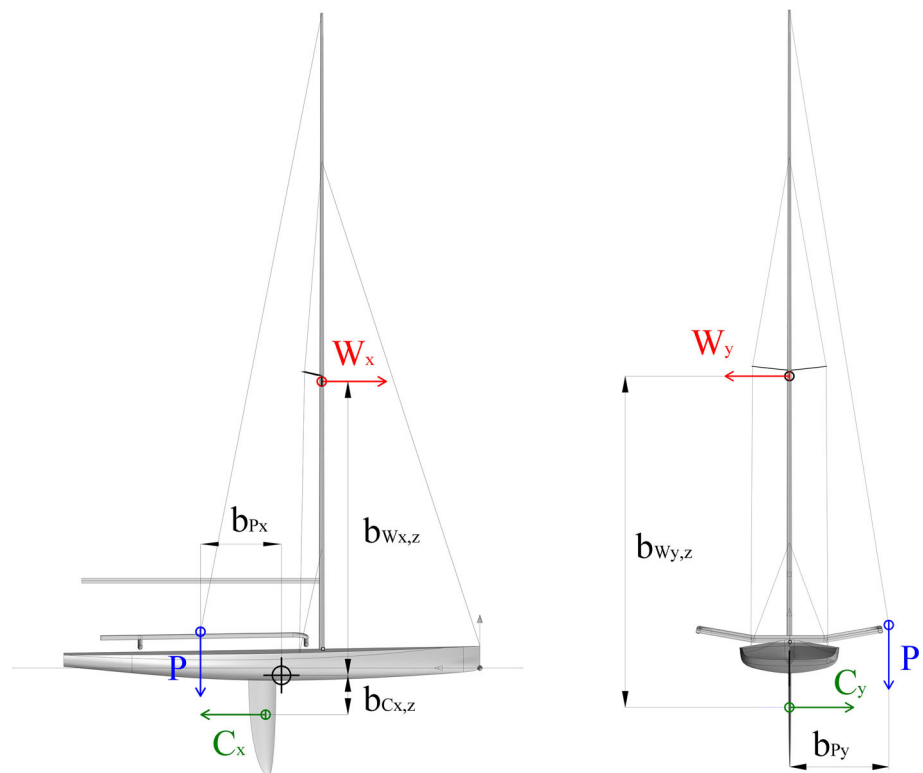

Fig. 6 Subdivision in blocks of the fluid domain (*left*) and a particular of the mesh (*right*)

3.2 CFD simulations

The evaluation of the external load system during navigation given in Sect. 3.1 follows from several procedural assumptions stated above. A different approach for the aerodynamic load estimation is now used in order to validate the results of Table 1. Computational fluid dynamics (CFD) analyses have been performed on the sails with the Fluent module of ANSYS. In particular, an approach close to the one described in [22] has been adopted. An hexahedral mapped mesh, structured in 60 blocks shown in Fig. 6 left, has been modelled with ICEM-CFD. With respect to a characteristic length, c, (in this case the chord of the main sail at the base which is

roughly 2 m) the domain extension is $20c$, $20c$ and $6c$ in the x, y and z direction respectively.

The close up of Fig. 6 right shows the surface mesh. Care has been taken in meshing the channel between the main sail and the jib in order to better approximate the interference phenomena. Moreover, such kind of topology can easily manage parametric analyses obtained by changing some variables (like for instance jib and main sail angles). A detailed description of the analysed configuration can be found in [1]. For the purpose of this work the jib angle and the apparent wind direction have been fixed at 9 and 20° respectively while four different apparent wind velocities have been simulated (3, 5, 7 and 9 m/s).

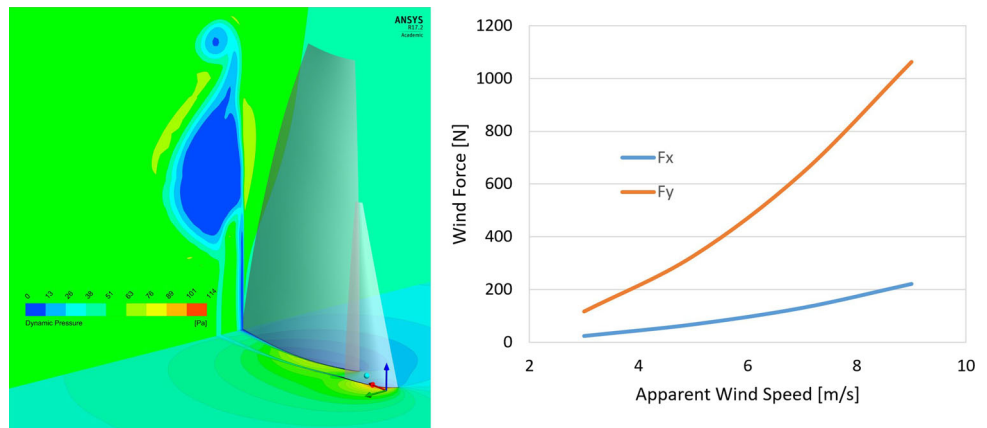**Fig. 7** Dynamic pressure map at 9 m/s (*left*) and wind force components from CFD (*right*)

Figure 7 left, shows the dynamic pressure map corresponding to the higher wind velocity (9 m/s) plotted on the plane $z = 3$ m and on the plane immediately behind the main leech. By calculating the resultant of the dynamic pressure on the sails, the two components of the wind force along x and y directions have been determined and plotted in Fig. 7 right versus the wind speed.

By observing Fig. 7 right, it can be noted that in correspondence of a wind speed of 8.5 m/s, the wind force components are $W_x = 200$ N and $W_y = 950$ N. These values are fairly close to those obtained by solving Eqs. (1) and (2). The simple analytical solution proposed in Sect. 3.1 can be then considered as a valid and time saving approach to evaluate the wind forces acting on the boat during navigation.

3.3 FEM model

The CAD model of the boat has been imported from CREO in the ANSYS Workbench environment. In order to numerically model the elastic behaviour of a composite sandwich, different approaches can be followed: solid or shell elements can be used to model each orthotropic lamina of the composite sandwich [23] or a single lamina with an equivalent material can be assumed to simulate the global stiffness of the sandwich. For an accurate determination of the strain status of each lamina constituting the sandwich, in this paper the material has been defined using the ANSYS ACP Pre-Post, where the elastic orthotropic properties are assigned to the unidirectional patch and then the stacking sequence of all laminae is defined to the model surfaces. The orthotropy of the material defined in the ACP module is associated to a linear elastic constitutive model implemented in the APDL solver. The mechanical characterization of the flax composite skin and the cork core has been performed in previous works [18,19]. The sequence used in the sandwich panels is [0/45/-45/90/cork/90/-45/45/0]. The symmetry is defined to the whole sandwich and not to the single skin. Direction 0° is aligned with the longitudinal x axis (see Fig. 8). In Fig. 8,

green arrows indicate the fibre orientation of the laminae for the skin layup. All other components of the boat, i.e. web frames, keel, trunk and deck, are made of isotropic marine plywood.

The element type used for the FE model is the four-noded SHELL181, with membrane plus flexural behaviour. In the case of components made of marine plywood, the element has a specified thickness, while, for the sandwich hull, is associated to a layered section. All connections between components are simulated with perfectly bonded edge to edge contacts. Average dimension of the element side is approximately 10 mm. Some mesh refinements are defined in the areas where resistance gauges are located, see Fig. 9 left. Loads applied to the model are shown in Fig. 9 right, where red arrows indicate punctual forces given by shrouds, mast, forestay and terrace while the coloured contour indicate the hydrostatic pressure distribution.

Concerning about the external constraints of the FEM model, displacements along x must be inhibited in order to equilibrate W_x. The heeling moments along y given by W_y and P are equilibrated by the reactions caused by the constrains along y on the vertical surfaces of the trunk. Simple supports in the vertical direction have also been inserted at bow and stern in the longitudinal plane to enhance the analysis convergence; in fact, small numerical differences between the resultant of the external forces and the resultant of the hydrostatic pressure could lead to undesired rigid body motion.

3.4 Numerical-experimental comparison

Strain values, measured from ERs (see Sect. 2) under the only action of rigging loads, are used for the validation of the FEM model. The boat has been rigged in the laboratory at different preload levels and in two different configurations (with and without the deck). Rigging loads up to 1600 N (measured on the shrouds by load cells and reported in Table 1) were applied, and ER data were observed to grow linearly within this range of loads.
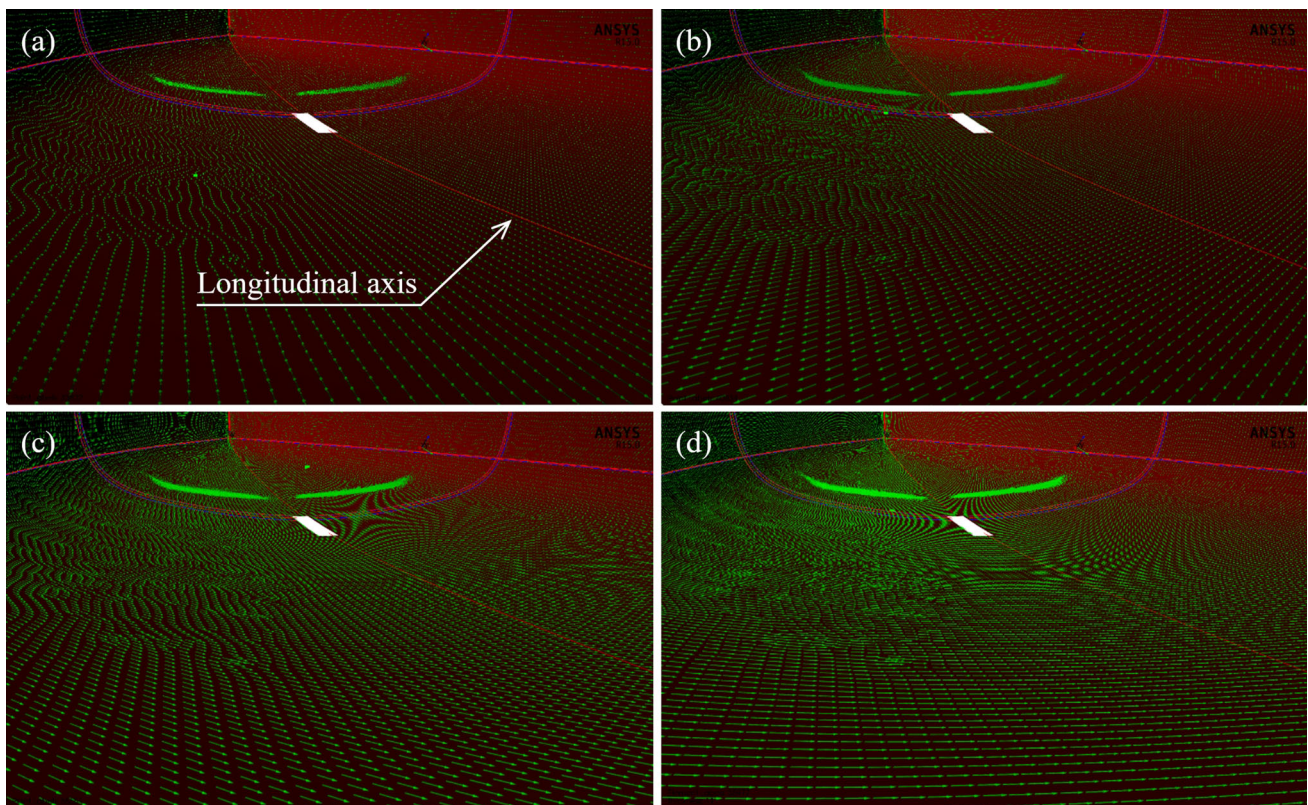
Fig. 8 Fibre orientation of the unidirectional lamina of the skin with respect to the longitudinal keel axis defined in the ACP module: **a** 0°, **b** 45°, **c** −45° and **d** 90°
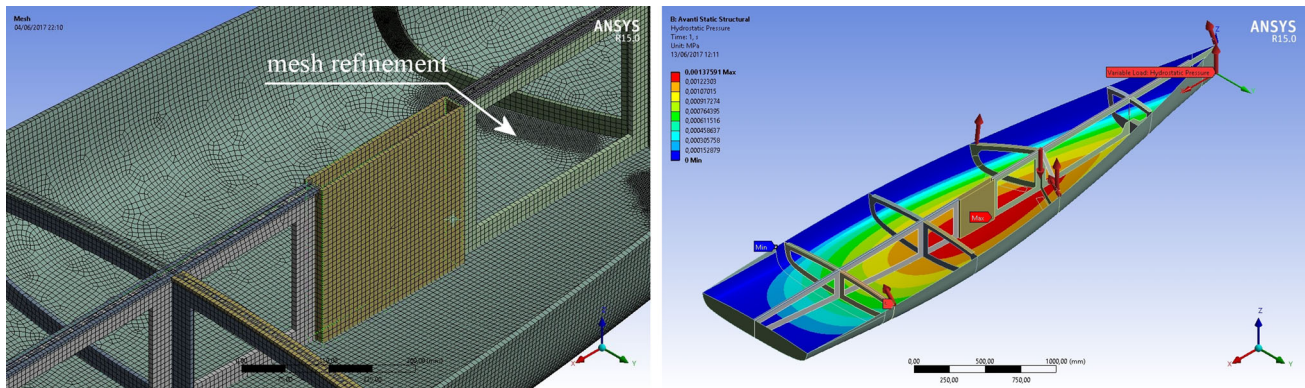

Fig. 9 View of the mesh (*left*) and applied loads (punctual and distributed) on the model (*right*)

To numerically calculate strain values in the positions where ERs are applied, several user coordinate systems are created in ANSYS in the corresponding locations (see Fig. 4). The deformation values predicted by the FEM model are calculated along the directions corresponding to the ERs grid orientations. An example of calculation of single grid strain measurement is reported in Fig. 10 left where it can be observed the map of the strain in the grid axis direction of SWP on the transversal reinforcement. The origin of the local system is the location of the strain gauge. In the same figure, a relevant strain concentration is evident in the inner portion of the reinforcement, in the area where the cross section of the hull has a high change of curvature.

A similar procedure is followed for strain evaluation in correspondence of the rosettes: values are numerically calculated in the inner lamina of the sandwich along the directions of the three grids of each rosette and then post processed in order to determine the principal strains. As previously observed, the principal strain is less sensitive to possible installation errors and a more confident comparison can be carried out between numerical and experimental results.
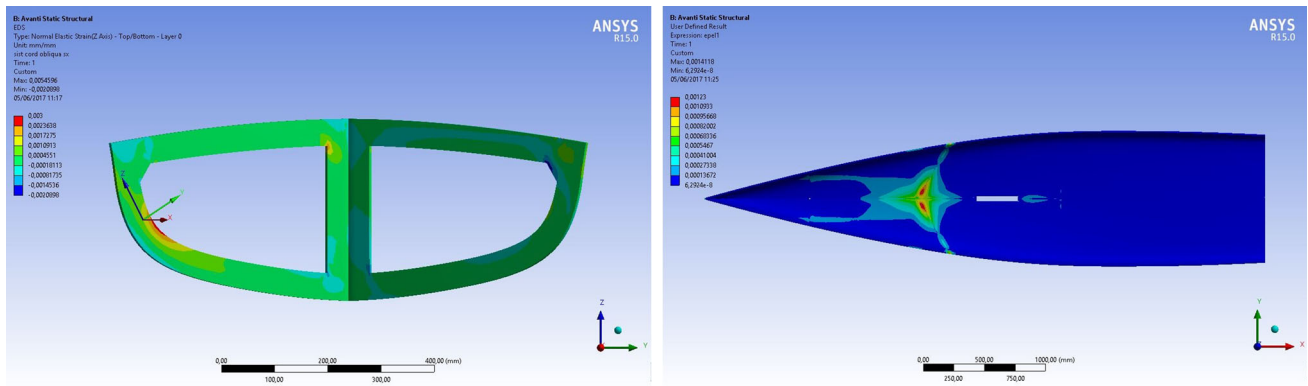
Fig. 10 Contour map of the normal strain aligned with the SWP grid (*left*) and contour map of the maximum principal strain on the upper in-board lamina of the hull (*right*)

Table 2 Comparison between strain measurements (µm/m) obtained with experiments and FEM

Configuration	Method	SKS	SKP	SWS	SWP	RBS	RBP	RSS	RSP
Rigging 1	Experiments	508	434	2474	2100	319	276	245	194
	FEM	465	396	2190	1997	327	325	245	228
	Error %	8.5	8.8	11.5	4.9	−2.6	−17.8	−0.3	−17.5
Rigging 2	Experiments	311	256	1276	1144	–	–	–	–
	FEM	310	270	1310	1220	–	–	–	–
	Error %	0.3	−5.5	−2.7	−6.6	–	–	–	–

Figure 10 right shows the map of the principal strain on the inner lamina of the sandwich hull. It can be observed that the rigging preload has effects only in the front half of the boat: the most deformed area is located around the mast foot and, in general, at the joints between the wood web frames and the hull sandwich.

Experimental and numerical strains for the two configurations with and without deck are compared in Table 2. For the Rigging 2 case, only measurements coming from single grids have been acquired because of setup problems. A good agreement can be generally noted, especially for the single grid ERs. In the worst case, the maximum difference does not exceed 18%. In fact, although the experimental setup was designed trying to foresee and control many potential sources of error, the complexity of the structure still exposes the experimental campaign to several uncertainties. In order to monitor the more severe strains, gauges have been located in areas of high strains, but these areas are generally characterised by high strain gradients. As a consequence, little mismatches between the actual physical positions of ERs in the boat and the corresponding position in the FEM model can determine significant differences between the respective strains. Further sources of uncertainties may regard the actual extent of symmetry and symmetrical behaviour of the real boat, the presence of internal defects such as delaminations or dry spots in the sandwich, approximations in the elastic constitutive behaviour of all the materials involved, etc... In

light of all these factors, the extent of errors shown in Table 2 is considered as widely tolerable.

4 Numerical prediction of navigation

Profiting from the positive comparison between experimental and numerical result commented in Sect. 3, it can be assumed that the FEM model can provide reliable results in terms of boat behaviour, also in other loading scenarios. Based on such assumption, some different loading conditions have been numerically investigated, in order to evaluate the boat behaviour under more complex navigation conditions, which are otherwise difficult to reproduce and monitor in lab environments.

In particular four loading scenarios have been considered, which are schematically represented in Fig. 11:

– C1: pure rigging load with the load on shrouds equal to 1600 N;
– C2: the boat floats on flat sea, and is subject to the rigging loads, the hydrostatic pressure and the loads from the crew, imagined as sited on the centre of the deck;
– C3: the boat navigates on flat sea, and is subject to the rigging loads, hydrostatic and aerodynamic pressure, and the weight of the crew, now imagined as positioned on trapeze;
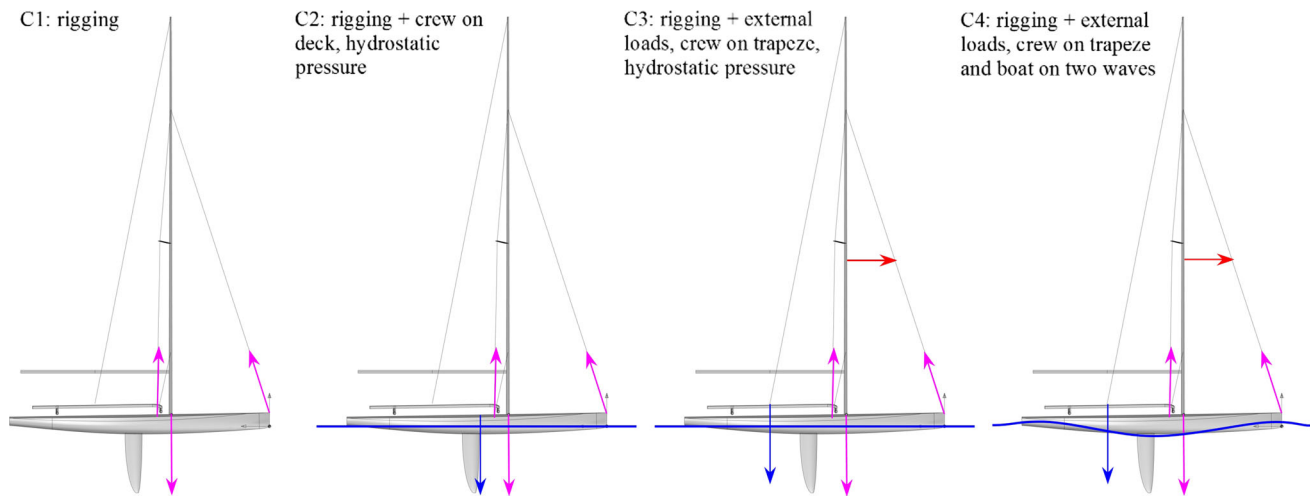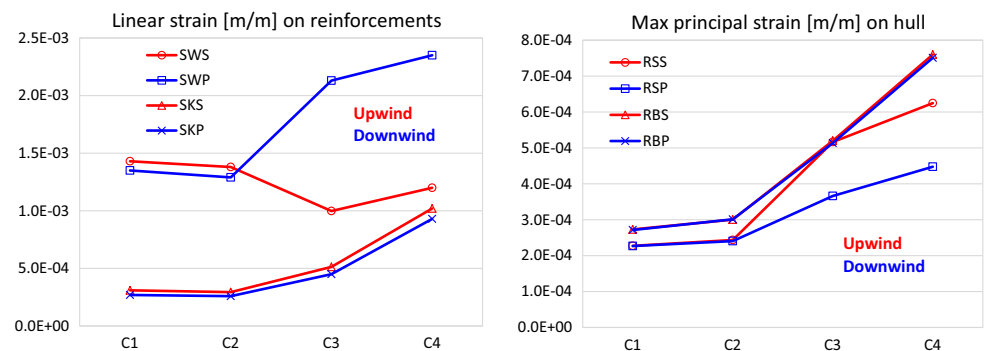
Fig. 11 Load configurations for numerical prediction during navigation

Fig. 12 Diagrams of strain levels predicted by FEM at ER locations during navigation

– C4: the boat navigates on rough sea, with loads due to rigging, and is subject to the rigging loads, aerodynamic pressure, and the weight of the crew on trapeze.

An hydrostatic pressure is applied on the hull in configuration C2 and C3, while in configuration C4 the model is supported only at bow and stern as on two wave peaks. Diagrams in Fig. 12 summarize results obtained from FEM simulations in terms of the strains that would be measured by the installed ERs. The upwind side corresponds to the starboard and the downwind side to the port.

With regards to single grid ERs (Fig. 12 left) the following considerations can be done. Strains calculated on the keel (SKS and SKP) are very similar at starboard and at port side, and are sensitive to the load configuration: maximum strain is calculated at C4 and is four time the one calculated at C1 (1.0 vs. 0.25 m/m). On the contrary, strains calculated on the web frame have a very different behaviour at starboard and port side depending on the load configuration. At C1 and C2 no significant change can be observed between SWS and SWP; when C3 and C4 are considered, the curves split into different directions: SWP (downwind) shows an increase of the strain with respect to SWS (upwind). It can be generally observed that, for this kind of boats, during navigation the weight of the crew on trapeze requires an increase of the load given by the downwind shroud, associated with a decrease of the load given by the upwind shroud.

With regards to rosettes (Fig. 12 right) the following considerations can be done. The strain level always increase from configuration C1–C4. RBS and RBP are substantially overlapped in each load configuration, this means that the hull panels ahead of the mast have a symmetric strain level. Behind the mast, RSS and RSP have equal deformations only at C1 and C2 but during navigation (C3 and C4) the increase in the strain level is more consistent in the upwind side (RSS).

Finally, attention has been focused on the macroscopic displacement of some key points of the hull under loading. In particular, two areas exhibits large displacements as depicted in Fig. 13. The z-component of displacement is mapped in Fig. 13 left for configuration C1: the area in blue is subjected to a lowering of 2.95 mm with respect to the design shape. This is caused by the high compression load carried by the foot mast. The y-component of displacement is mapped in Fig. 13 right for configuration C1: the blue and red areas become closer to the keel line due to the y-component of the
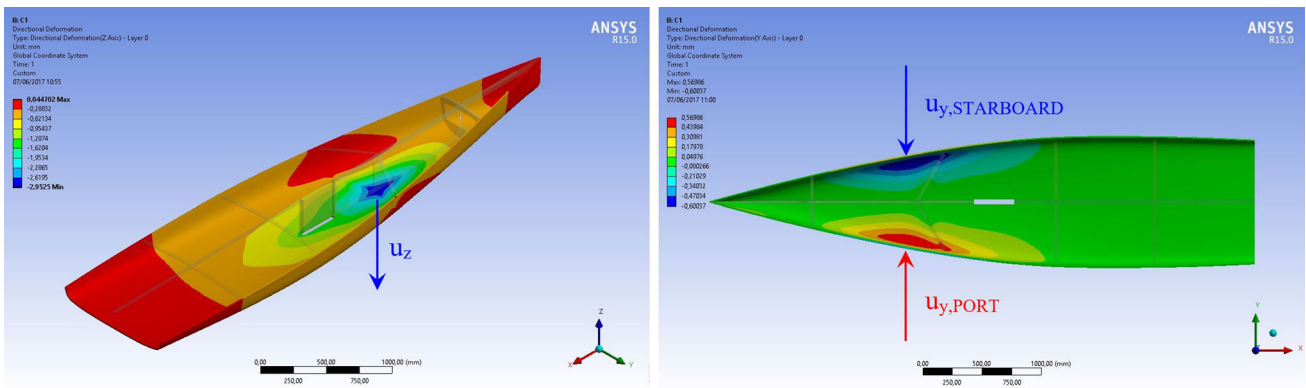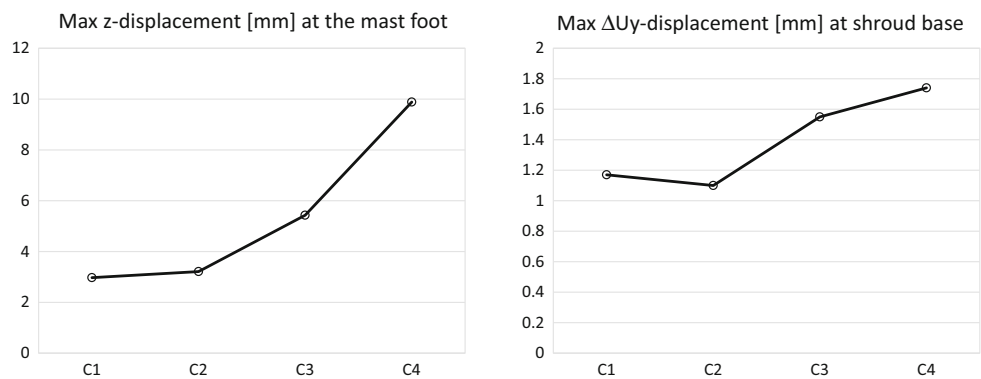
Fig. 13 Displacement of the hull for configuration C1 along z (*left*) and along y (*right*)

Fig. 14 Diagrams of displacements predicted by FEM

load on shrouds. It results in a reduction of the distance in y between the shroud bases of 1.15 mm.

Same calculations have been performed for the other loading configurations and results are summarized in Fig. 14. The displacement along z under the mast foot can be observed in Fig. 14 left where a maximum value of 9.9 mm is evaluated for configuration C4. This result demonstrates that the shape of the hull (and the related water lines) can undergo relevant modifications in navigation conditions. A minor issue is the change of the distance in y between the shroud bases reported in Fig. 14 right, that never exceeds 1.8 mm.

5 Conclusions

A numerical procedure has been described in this work where the CAD model of an existent sailing dinghy has been used to assess the feasibility of a shape refitting and to study the strain state via FEM simulations. The boat has been entirely manufactured in laboratory and is composed by an internal web frame made of marine plywood and by sandwich panels for the deck and the hull made of a hybrid eco-sustainable material. This sandwich is constituted by external flax fibre reinforced-epoxy skins and by an internal cork core. From previous mechanical characterization activities, an accurate elastic constitutive model of the material has been implemented in the FEM code.

To validate the reliability of this numerical procedure, the refitted boat has been instrumented with single and three grid electrical resistance gauges, located in those areas of the boat where preliminary FEM simulations give relevant strain levels. A numerical-experimental comparison between ERs strains and the equivalent numerical strains has been performed with the boat subject to a symmetric rigging load. The comparison was performed on different locations in the hull and wooden frame, and all analysed sites provided experimental and numerical values differing at most by 18%. This is considered a fairly good agreement, given the complexity of the structure, of the materials involved and the approximations needed to schematically represent the loadings. In light of this successful comparison, it can be concluded that the proposed FEM model can be confidently used to optimize the structure towards more complex loading scenarios.

Then, real navigation configurations have been also simulated with the aim to predict the strain level of the boat in close-hauled on flat and rough sea. It has been remarked that the maximum strain level during navigation can double the one estimated after the preload on the rig, in particular in the downwind side of the boat. Furthermore, a maximum displacement of about 10 mm has been predicted in the vertical

direction under the mast foot when the boat is between two wave peaks. This phenomenon involves a relevant modification of the waterlines of the boat and should be carefully approached in the design phase by means of fluid-structure interaction procedures.

Future work will attempt to use the installed strain gauges to measure strains during navigation conditions, in order to provide further confirmation of the effectiveness of the FEM model and to work as a real time monitoring system of the overall behaviour of the boat.

References

1. Ingrassia, T., Mancuso, A., Nigrelli, V., Tumino, D.: A multi-technique simultaneous approach for the design of a sailing yacht. Int. J. Interact. Des. Manuf. **11**, 19–30 (2017)

2. Cappello, F., Ingrassia, T., Mancuso, A., Nigrelli, V.: Methodical redesign of a semitrailer. WIT Trans. Built Environ. **80**, 359–369 (2005)

3. Biancolini, M.E., Viola, I.M., Riotte, M.: Sails trim optimisation using CFD and RBF mesh morphing. Comput. Fluids **93**, 46–60 (2014)

4. Allen, T., Battley, M., Casari, P., Kerling, B., Stenius, I., West-lund, J.: Structural responses of high performance sailing yachts to slamming loads. In: 11th International Conference on Fast Sea Transportation FAST, Honolulu, Hawaii, USA (2014)

5. Kelly, D., Reidsema, C., Bassandeh, A., Pearce, G., Lee, M.: On interpreting load paths and identifying a load bearing topology from finite element analysis. Finite Elem. Anal. Des. **47**, 867–876 (2011)

6. Lee, M.C.W., Payne, R.M., Kelly, D.W., Thomson, R.S.: Determination of robustness for a stiffened composite structure using stochastic analysis. Compos. Struct. **86**, 78–84 (2008)

7. Ocera, M., Boote, D., Vergassola, G., Faloci, F.: Simplified analytical method for the evaluation of longitudinal strength of large sailing yachts. Ocean Eng. **133**, 182–196 (2017)

8. Rizzo, C.M., Boote, D.: Scantling of mast and rigging of sail boats: a few hints from a test case to develop improved design procedures. 11th International Symposium on Practical Design of Ships and Other Floating Structures Rio de Janeiro, RJ, Brazil (2010)

9. Zamarin, A., Matulja, T., Hadjina, M.: Methodology for optimal mast and standing rigging selection of a racing yacht using AHP and FEM. Brodogradnja **64**, 11–21 (2013)

10. Murayama, H., Wada, D., Igawa, H.: Structural health monitoring by using fiber-optic distributed strain sensors with high spatial resolution. Photon. Sens. **3**(4), 355–376 (2013)

11. Day, A.H.: Performance prediction for sailing dinghies. Ocean Eng. **136**, 67–79 (2017)

12. Pennanen, M., Levin, R.L., Larsson, L., Finnsgård, C.: Numerical prediction of the best heel and trim of a Laser dinghy. Procedia Eng. **147**, 336–341 (2016)

13. Banks, J., Marimon Giovannetti, L., Taylor, J.C., Turnock, S.R.: Assessing human-fluid-structure interaction for the international moth. Procedia Eng. **147**, 311–316 (2016)

14. Ingrassia, T., Nalbone, L., Nigrelli, V., Ricotta, V., Pisciotta, D.: Biomechanical analysis of the humeral tray positioning in reverse shoulder arthroplasty design. Int. J. Interact. Des. Manuf. (2017). doi:10.1007/s12008-017-0418-8

15. Ingrassia, T., Mancuso, A., Nigrelli, V., Tumino, D.: Numerical study of the components positioning influence on the stability of a reverse shoulder prosthesis. Int. J. Interact. Des. Manuf. **8**(3), 187–197 (2014)

16. Ajovalasit, A., Cipolla, N., Mancuso, A.: Strain measurement on composites: errors due to rosette misalignment. Strain **38**, 150–156 (2002)

17. Ajovalasit, A., Pitarresi, G.: Strain measurement on composites: effects due to strain gauge misalignment. Strain **47**(SUPPL. 1), e84–e92 (2011)

18. Mancuso, A., Pitarresi, G., Tumino, D.: Mechanical behaviour of a green sandwich made of flax reinforced polymer facings and cork core. Procedia Eng. **109**, 144–153 (2015)

19. Pitarresi, G., Tumino, D., Mancuso, A.: Thermo-mechanical behaviour of flax-fibre reinforced epoxy laminates for industrial applications. Materials **8**(11), 7371–7388 (2015)

20. Larsson, L., Eliasson, R.E.: Principles of Yacht Design. Adlard Coles Nautical, London (1996)

21. Bamett, A.R., Widrick, T.W. Ludwiczak, D.R.: Closed-Form Static Analysis With Inertia Relief and Displacement-Dependent Loads Using a MSC/NASTRAN DMAP Alter. NASA TM 106836 (1995)

22. Kim, W.-J., Yoo, J., Chen, Z., Rhee, S.H., Chi, H.-R., Ahn, H.: Hydro- and aerodynamic analysis for the design of a sailing yacht. J. Mar. Sci. Technol. **15**(3), 230–241 (2010)

23. Ye, Y., Chen, C., Liu, X.: Structural strength analysis of FRP yacht by FEM. Appl. Mech. Mater. **275–277**, 105–110 (2013)